JACS
JOURNAL OF THE AMERICAN CHEMICAL SOCIETY

Article

pubs.acs.org/JACS

A Simple Road for the Transformation of Few-Layer Graphene into MWNTs

Mildred Quintana,*[,†,⊥] Marek Grzelczak,[†] Konstantinos Spyrou,[‡] Matteo Calvaresi,[§] Sara Bals,[∥] Bart Kooi,[‡] Gustaaf Van Tendeloo,[∥] Petra Rudolf,*[,‡] Francesco Zerbetto,*[,§] and Maurizio Prato*[,†]

[†]Center of Excellence for Nanostructured Materials (CENMAT) and INSTM, unit of Trieste, Dipartimento di Scienze Chimiche e Farmaceutiche, University of Trieste, Piazzale Europa 1, I-34127 Trieste, Italy

[‡]Zernike Institute for Advanced Materials, University of Groningen, Nijenborgh 4, NL-9747AG Groningen, The Netherlands

[§]Dipartimento di Chimica "G. Ciamician", Università di Bologna, V. F. Selmi 2, 40126 Bologna, Italy

[∥]EMAT, University of Antwerp, Groenenborgerlaan 171, B-2020 Antwerp, Belgium

Supporting Information

ABSTRACT: We report the direct formation of multiwalled carbon nanotubes (MWNT) by ultrasonication of graphite in dimethylformamide (DMF) upon addition of ferrocene aldehyde (Fc-CHO). The tubular structures appear exclusively at the edges of graphene layers and contain Fe clusters. Fc in conjunction with benzyl aldehyde, or other Fc derivatives, does not induce formation of NT. Higher amounts of Fc-CHO added to the dispersion do not increase significantly MWNT formation. Increasing the temperature reduces the amount of formation of MWNTs and shows the key role of ultrasound-induced cavitation energy. It is concluded that Fc-CHO first reduces the concentration of radical reactive species that slice graphene into small moieties, localizes itself at the edges of graphene, templates the rolling up of a sheet to form a nanoscroll, where it remains trapped, and finally accepts and donates unpaired electron to the graphene edges and converts the less stable scroll into a MWNT. This new methodology matches the long held notion that CNTs are rolled up graphene layers. The proposed mechanism is general and will lead to control the production of carbon nanostructures by simple ultrasonication treatments.

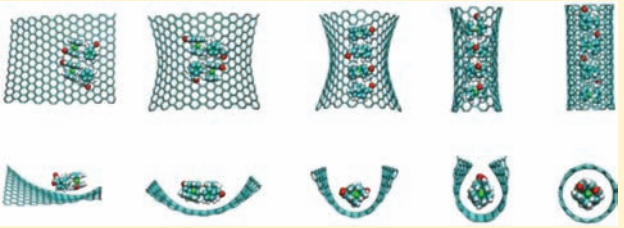

INTRODUCTION

Carbon is a most versatile element that occurs in allotropic forms as diverse as diamond and graphite and in the more recently discovered nanostructures of fullerenes, nanotubes (CNTs), and graphene.[1] The production of graphene by micromechanical cleavage[2] triggered enormous experimental activity. Many studies demonstrated that graphene monolayers possess novel structural,[3] electrical,[4] and mechanical[5] properties. Additionally, graphene can be thought as a 2D building block for carbon nanostructures of other dimensionalities. It can be wrapped into 0D buckyballs, rolled into 1D nanotubes, or stacked into 3D graphite.[6] Recently, in situ TEM experiments demonstrated the direct transformation of flat graphene sheets into fullerene cages where etching of the edge carbon atoms promotes folding into fullerenes.[7]

CNTs are often described as rolled-up graphene layers. Matching this concept to experiments where the layers fold into CNTs is still a great challenge. To date large-scale mass CNT production has only been achieved by stochastic synthetic processes, such as arc discharge,[8] laser ablation,[9] and chemical vapor deposition (CVD),[10] which require postsynthetic separation and purification treatments.[11]

During the past few years, ultrasonication has become an extremely powerful tool in the synthesis, modification, and manipulation of carbon nanomaterials.[12] Under appropriate conditions, ultrasounds can functionalize CNTs, open their caps, or even fracture them completely.[13] In addition to surface modifications, CNTs can be prepared directly from organic solvents with the assistance of ultrasounds.[14−16] Graphite ultrasonication produces exfoliation in many solvents, if the free energy of mixing is negative[17] and the solvent is able to stabilize colloidal graphene.[18] It is accepted that ultrasounds break the graphitic basal structure and produce graphitic carbon fragments of variable sizes, which are later intercalated by solvent molecules.[19] To complicate matters, ultrasounds generate cavities whose implosion releases sufficient energy to form high-energy intermediates and free radicals that can drive chemical reactions.[20,21] Chemical attack reduces the size of the graphene sheets and is therefore detrimental to the physical properties that are usually sought after. Graphene dispersions produced by exfoliation of graphite in organic solvents, such as *N*-methyl-2-pyrrolidone (NMP) and *N*,*N*-dimethylformamide (DMF), first reached concentrations up to 0.01 mg/mL and 1 wt % monolayer.[17] Increasing sonication time, the concentration increased up to 1.2 mg/mL and 4 wt% monolayer.[22]

Received: April 1, 2012
Published: May 7, 2012

   dx.doi.org/10.1021/ja303131j | J. Am. Chem. Soc. 2012, 134, 13310−13315

The resulting graphene sheets presented higher concentration of defects and size reduction proportional to the sonication time. Previous studies demonstrated that sonication in DMF produces $\cdot CH_3$ and $\cdot CH_2N(CH_3)CHO$ radicals.[23] These radicals form either through reaction of the solutes with ultrasound-generated ·H and ·OH radicals or by direct pyrolysis of weak bonds. In air-saturated sonicated solutions, the radicals convert to the corresponding peroxyl radicals, such as $\cdot OOCH_2N(\cdot CH_3)CHO$.[24] By virtue of their longer lifetimes and higher selectivity, the latter species are likely responsible for the damage of the graphene layers. To avoid oxidation, antioxidant molecules, for instance, natural flavonoids, can be employed to effectively inhibit the formation of the free radicals generated during sonication.[24]

RESULTS AND DISCUSSION

In the present work, we sonicated graphite in DMF in the presence of ferrocene aldehyde (Fc-CHO),[25] a reducing agent that can inhibit reactions promoted by oxygen, peroxides, and radicals. Ferrocene derivatives are used in the synthesis of CNTs as catalysts and carbon source.[26] Addition of Fc-CHO reduces the effect of long sonication times on graphene sheets and produces the controlled cutting of graphene sheets close to the edges. The direct formation of multiwalled carbon nanotubes (MWNT) is here observed for the first time. It occurs by sealing unstable pieces of graphene sheets of limited size.[26,27] A schematic representation of the experimental procedure is presented in Figure 1.

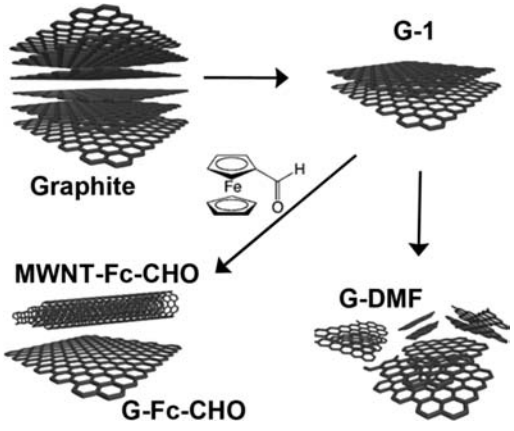

Figure 1. Ultrasound-assisted synthesis of carbon nanostructures.

Samples were prepared using the ultrasonic tip processor GEX 750. All samples were sonicated in cycles of 30 s on/30 s off for 1 or 3 h periods of time at the lower power of the ultrasonic tip (20%, 112.5 W). During ultrasonication, samples were kept in an ice bath to avoid overheating. As a starting material, we produced G-1: 10 mg of graphite crystals were ultrasonicated in 30 mL of DMF during 1 h in order to induce partial exfoliation of graphite (see Experimental Section). UV–vis spectroscopy was used to measure the absorption at 660 nm. The concentration of the final dispersion was calculated using the absorption coefficient $\alpha = 2460$ mL/mg·m,[17] resulting in 0.031 ± 0.003 mg/mL. The dispersed material was investigated by transmission electron microscopy (TEM), Figure 2a. TEM analysis of G-1 (30 micrographs) indicates the presence of graphene flakes with lateral size of typically a few μm, consisting of several layers.

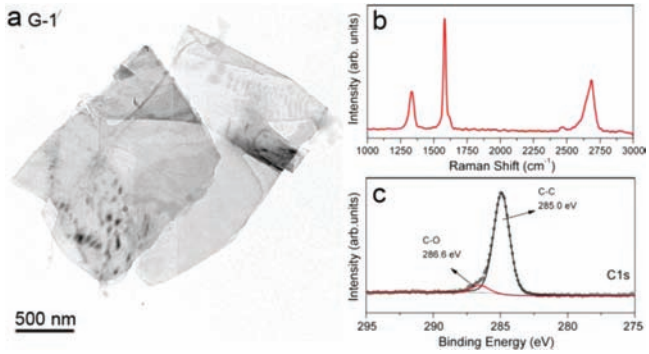

Figure 2. Starting material. TEM micrographs of solution cast G-1(a). Raman spectra excited at 633 nm for G-1 (b). C 1s core level region of the X-ray photoemission spectra of G-1 (c).

D-Fc-CHO was obtained by sonication of G-1 with the addition of Fc-CHO (Figure 3). After washing and redispersing

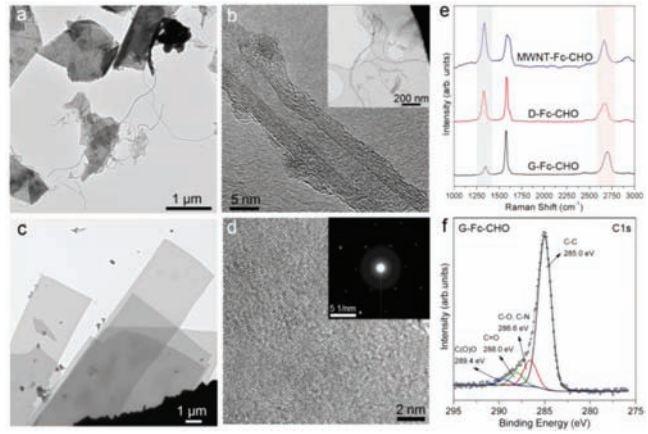

Figure 3. Carbon nanostructures produced by the addition of Fc-CHO during ultrasonication of G-1. (a) TEM micrograph of solution cast D-Fc-CHO. (b) HR-TEM of D-Fc-CHO where a MWNT on a graphene lattice is observed; in the inset, a panoramic TEM micrograph of MWNT-Fc-CHO is shown. (c) Representative TEM micrograph of G-Fc-CHO. (d) HR-TEM image of G-Fc-CHO; the inset shows the corresponding diffraction pattern. (e) Comparison of the Raman spectra of MWNT-Fc-CHO, D-Fc-CHO and G-Fc-CHO collected exciting at 633 nm, the D and 2D bands are highlighted. (f) C 1s core level photoemission line of G-Fc-CHO.

the product in 10 mL of fresh DMF, the concentration of the sample was calculated from the optical absorption, as described above for G-1, and found to be 0.029 ± 0.003 mg/mL. When analyzed by TEM, the presence of very long MWNTs (2 ± 0.5 μm) was observed in D-Fc-CHO, as shown in Figure 3a. The formation of the tubular structures is seen exclusively at the edges of graphene layers. (Supporting Information, SI-1).

Further analysis of the sample by HR-TEM, proved the existence MWNTs. In some micrographs it is possible to distinguish the rolling up of the graphene edges, while in others completely isolated MWNTs are seen (Supporting Information, SI-2). The Raman spectrum of D-Fc-CHO is shown in Figure 3e. The I_D/I_G value of 0.72 and the 2D band at 2666 cm^{-1} implies a disordered material. After centrifugation, the concentration of the supernatant was again calculated from the optical absorption to amount to 0.007 ± 0.002 mg/mL. TEM images of this supernatant, MWNT-Fc-CHO, show preponderantly the presence of MWNT, but small graphene fragments

dx.doi.org/10.1021/ja303131j | J. Am. Chem. Soc. 2012, 134, 13310–13315

are still noticeable (Supporting Information, SI-3). The tube surfaces observed by HR-TEM reveal semicrystalline MWNT showing disordered, distorted fringes surrounding the hollow core. The distance between the graphene sheets was found to be 0.35 ± 0.01 nm. These structures are similar to as-grown MWNT obtained by chemical vapor deposition before annealing (Figure 3b inset).[28] The HR-TEM of these structures after annealing at 500 °C for 30 min showed the symmetric, evenly spaced line patterns that have been interpreted as images of coaxial, nested graphitic tubes (Figure 3b).[29] Alternatively, the same images were attributed to graphitic scroll structures.[30] As previously reported, scroll segments, consisting of rolled-up graphene sheets, may coexist with nested tube segments inside a continuous tubular structure. The implication is that MWNTs originate during the sonication process from the scrolls by carbon−carbon bond rearrangement.[31]

Further characterization of the sample by Raman spectroscopy captured the fingerprint of different carbon nanostructure.[32] For MWNT-Fc-CHO, the symmetrical shape of the 2D peak (no shoulder as in graphite) was evidence of the existence of MWNTs, since the sample does not contain the perfect structure of crystalline graphite due to the strong curvature of small diameter nanotubes (Figure 3e). The I_D/I_G value of 1.36 agrees with the semicrystalline structure observed by HR-TEM. The concentration of the lower part of the dispersion, G-Fc-CHO, was 0.012 ± 0.003 mg/mL. When this sample was deposited on a TEM grid, graphene sheets with lateral size of few micrometers were found. A representative TEM micrograph is reported in Figure 3c, additional micrographs can be seen in Supporting Information, SI-4. HR-TEM characterization confirms the presence of crystalline graphene, which was later corroborated by the analysis of the electron diffraction patterns. An example of this, inset in Figure 3d, shows what appears to be a single graphene.[33] The occurrence of a small D band at 1346 cm^{-1} and the I_D/I_G value of 0.33 are attributed to the edges of the graphene sheets. The 2D band is symmetrical and roughly consists of one component, typical of monolayer or few-layer graphene (Figure 3e). The C1s core-level photoemission line of G-Fc-CHO, presented in Figure 3f, gives insight into the chemical composition of this material: it shows, apart from the main component at 285.0 eV binding energy assigned to the aromatic carbon (77.2 ± 1.3% of the total amount of carbon), also contributions from carbon singly bound to oxygen or nitrogen at 286.6 eV (13.2 ± 0.3% of the total amount of carbon) as well as from carbonyl at 288.0 eV and carboxyl groups at 289.4 eV binding energy. The latter amount is 6.6 ± 0.1% and 3.1 ± 0.1%, respectively, of the total amount of carbon. The O1s peak of D-Fc-CHO (SI-5) demonstrates the presence of different oxidation states of carbon after the reaction. The peak at 532.4 eV of binding energy is attributed to oxygen singly bound to carbon, while the peaks at 531.1 and 533.5 eV stem from carbonyl and carboxyl groups, respectively. A minor amount of Fe, about 0.3 at %, was identified and probably is due to residual iron, close to the edges.

To test the possibility of producing larger quantities of MWNT, we added larger amounts of ferrocene aldehyde to the initial dispersion. No significant additional MWNT formation was observed by TEM, and the treatment resulted in further oxidation of the sample as confirmed by Raman spectroscopy and XPS analysis. The implication is that the mechanism of formation of MWNTs entails an interaction of Fc-CHO with graphene layers that must reach a plateau in terms of concentration.

As a control experiment we sonicated G-1 without the addition of Fc-CHO under the same experimental conditions of G-Fc-CHO. Figures 4a,b display representative TEM and

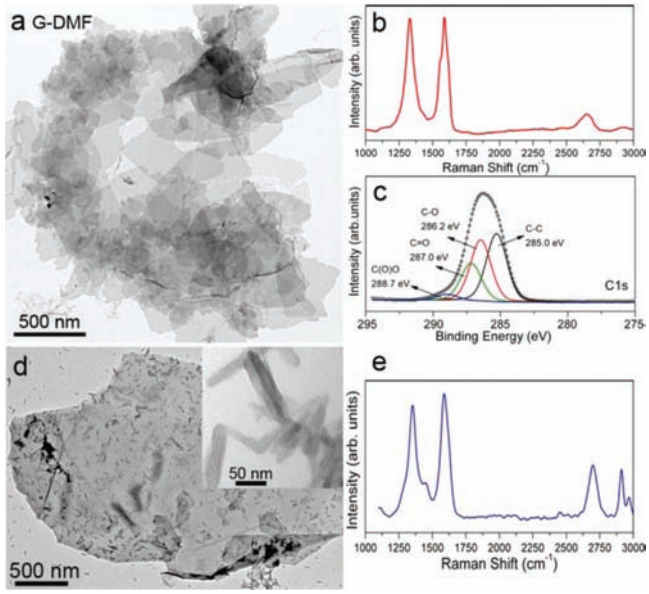

Figure 4. Control experiment performed by the sonication of G-1 without the addition of Fc-CHO (G-DMF): (a) TEM micrograph of drop-cast G-DMF, (b) Raman spectra of drop-cast G-DMF, and (c) C 1s core level photoemission line of G-DMF. Influence of temperature on the graphene exfoliation in the presence of the Fc-CHO. (d) G-Fc-CHO prepared by ultrasonication at room temperature. (e) Raman spectra of drop-cast G-Fc-CHO (room temperature) dispersion onto silicon oxide substrates, excited at 633 nm.

Raman spectra of G-DMF; the shape and intensity of the 2D band at 2650 cm^{-1} for G-DMF are significantly different from those of pristine graphite. Conversely, the 2D band of G-DMF shows a low-intensity band associated with damage of graphene.[34] The I_D/I_G value of 0.99 for G-DMF identifies the material as highly damaged graphene comparable to graphene oxide (GO).[35] Figure 4c shows the C1s core level photoemission lines of G-DMF. In the C1s line of G-DMF the component at 285.0 eV, due to aromatic carbon, is reduced to 41.6 ± 0.5%, while the C−O bonds at 286.2 eV account now for 34 ± 0.3% of the total carbon amount and smaller peaks at 287.8 eV (15.8 ± 0.2%) and 289.3 eV (8.5 ± 0.2%) are assigned to carbonyl and carboxyl groups, respectively. A slightly increased amount of nitrogen (2.5 at%) was also observed for G-DMF as compared to G-1 (Figure 2). Such an increase in the degree of oxidation of G-DMF may result from oxidative processes promoted by free radicals generated during ultrasonication. Hence, the addition of Fc-CHO minimizes the oxidation of G-1 treated under the same experimental conditions than G-DMF, decreasing the conversion of C−C bonds to other C−X species (X = O or N) by more than one-third. All the analyses identify D-Fc-CHO as a significantly less damaged material than G-DMF. From microscopy and Raman analysis, oxygenated groups are most abundant in the MWNT-Fc-CHO sample.

Five other control experiments were carried out. In the same conditions of ultrasonication, they used (i) Fc, (ii) benzaldehyde, (iii) Fc together with benzaldehyde, (iv) Fc-

dx.doi.org/10.1021/ja303131j | J. Am. Chem. Soc. 2012, 134, 13310−13315

COOH, and (v) $FcCON(CH_3)_2$. MWNTs were not observed in the reaction mixture in any of the cases. The experimental details and the characterization of the products in these control experiments are reported in the Supporting Information (SI-6−10).

The key role of the cavitation energy in these processes is demonstrated by increasing the temperature of the process to room temperature (25 °C). After ultrasonication of the G-Fc-CHO dispersion, we did observe the formation of carbon nanoscroll-like structures, Figures 4d and 4e, but not of MWNTs. The lack of formation of MWNTs is due to the fact that the higher temperature decreases the energy density of cavitation[36] and allows terminal radical reaction pathways to dominate.

The experimental findings together with the control experiments allow us to conceive a possible mechanism for the formation of carbon nanotubes based on the multiple role of FcCHO. Defects caused by various factors, including chemical functionalization[37] or physical adsorption,[38] play a crucial role in the spontaneous twisting and folding and in the disruption of the aromatic bond network of graphene nanoribbons.[39] Rolling of the sheets starts from the edges[40,41] and entails an energy barrier that must be overcome. Fc-CHO templates the formation of MWNT by lowering the barrier for rolling nanoribbons. Incapsulation of metallocene molecules in nanotubes is a highly exothermic process.[42] Formation of ferrocene nanorods, attributed to $\pi-\pi$ stacking of ferrocene molecules, on the surface of graphene sheets has been observed experimentally.[43] We performed a combination of molecular mechanics and molecular dynamics calculations for an increasing number of Fc-CHO molecules deposited on the nanoribbon obtained by unzipping a (8,8) CNT (see Table SI-1 and SI-11, Supporting Information). The length of the tube was 24.5 Å. In the absence of Fc-CHO, the activation barrier for folding the nanoribbon is 120.3 kcal mol^{-1}. Introduction of the first Fc-CHO molecule decreases the barrier by 17.8 kcal mol^{-1}. The energy decrease is further lowered by the introduction of each subsequent Fc-CHO molecule. When 4 Fc-CHOs template the process, the barrier is nearly halved to 63.3 kcal mol^{-1}.

Crucial for templating the folding of graphene sheets by Fc-CHO is the presence of iron inside the MWNTs, as detected by TEM (SI-13, Supporting Information). It confirms that incorporation of Fc-CHO occurs and strongly vouches for their templating activity and supports the idea that this is the starting mechanism in the formation of the MWNT.

In the five control experiments, MWNTs were not observed in the reaction mixture. Fc, benzaldehyde, Fc together with benzaldehyde, Fc-COOH, and $FcCON(CH_3)_2$ may still be able to exert in some templating activity or roll up the sheets but must lack part of the properties of Fc-CHO that produce MWNTs.

We performed quantum chemical calculations (Table SI-2, Supporting Information) that showed that Fc-CHO has the highest electron affinity (EA) of a set of molecules that comprised also Fc-COOH, Fc-$CON(CH_3)_2$, Fc, and benzaldehyde. Since Fc-CHO is the only molecule that produces CNTs, these calculations confirm that its radical scavenging activity is superior to that of the others and can be of primary importance in the MWNT formation. The large spin density located on the aldehydic group of Fc-CHO (Figure SI-14, Supporting Information) further shows its role in the antioxidant activity.

A final feature to consider is that in graphene, the reactivity of edges is at least twice as large as the reactivity of the bulk atoms.[44] This observation concurs with scanning tunneling spectroscopy measurements that evidenced a higher electronic density of states near the Fermi level at the edges[45] and theoretical calculations that predicted that edge states occur in any graphene sheet.[46]

From all these observations, we suggest that during ultrasonication different scenarios may occur:

(i) In the absence of antioxidants, the radical species are strong enough to oxidize the graphene sheet; this process starts at the edges and at inner defects and slices graphene sheets in small pieces.
(ii) In the presence of Fc-CHO, the concentration of radical reactive species is considerably reduced; some radical attacks to the edges still occur and loosen the sheets.
(iii) Fc-CHO then acts in a different way; it localizes itself at the edges of graphene and templates the rolling up of a sheet to form a nanoscroll where it remains trapped; the localization implies that a limiting number of Fc-CHO can roll up the sheet, in agreement with the experimental finding that higher amounts of ferrocene aldehyde do not provoke additional MWNT formation.
(iv) Fc-CHOs inside the scroll then act as active bumpers in a pinball machine; they accept and donate unpaired electrons with the graphene edges and convert the less stable scroll into a MWNT.

While step (iv) is only putative, it makes chemical sense. This mechanism explains the formation of long tubes during the ultrasonication process.

■ CONCLUSION

Summarizing, the effect of adding Fc-CHO during exfoliation of graphite by ultrasonication in DMF was investigated. The formation of MWNTs was observed when this antioxidant was added. A considerable reduction in the degree of oxidation of the exfoliated graphene sheets was demonstrated by XPS and Raman spectroscopy analyses. Higher concentrations were determined, from the UV−vis absorption at 660 nm, of the dispersions, and larger graphene sheets were observed by TEM and HR-TEM. Our results allow us to propose a radical attack mechanism controlled by the presence of the antioxidant molecules and the different reactivity of diverse graphene edges. Templating activity of Fc-CHO facilitates the nanoribbons rolling. These results are expected to be useful in understanding how solvents disperse graphene and in advancing the controlled synthesis of carbon nanotubes. This procedure can also reach higher yields of liquid-phase exfoliation graphene.

■ EXPERIMENTAL SECTION

Characterization Techniques. The optical characterization was carried out by UV−vis NIR spectroscopy with a Cary 5000 spectrophotometer using 10 mm path length quartz cuvettes. TEM measurements were performed with a TEM Philips EM208, using an accelerating voltage of 100 kV. Samples were prepared by drop casting from the dispersion onto a TEM grid (200 mesh, nickel, carbon only). HR-TEM was performed with a JEOL 2010F operating at an accelerating voltage of 200 kV (point resolution 2.3 Å and information limit 1.1 Å). An aberration corrected TEM (FEI TITAN 50-80) was used at 120 kV in order to avoid beam damage during imaging. XPS data were collected using an SSX-100 (Surface Science Instruments) spectrometer equipped with a monochromatic Al Kα X-ray source ($h\nu$ = 1486.6 eV); the photoelectron take off angle was 37°, and the energy

resolution was set to 1.26 eV. The base pressure during the measurement was 3×10^{-10} mbar. Binding energies were referenced to the C1s core level for the C−C bond set to the nominal value of 285.0 eV.[47] Spectral analysis included a Shirley background subtraction and peak separation using mixed Gaussian−Lorentzian functions in a least-squares curve-fitting program (Winspec) developed in the LISE laboratory of the University of Namur, Belgium. The photoemission peak areas of each element, used to estimate the amount of each species on the surface, were normalized by the element-specific sensitivity factors tabulated for the spectrometer used. The substrates were evaporated gold films supported on mica (cleaned in an ozone discharge for 15 min, followed by sonication in ethanol for 20 min immediately before being employed). The samples were dispersed by sonication in a bath ultrasonicator, and then a drop was cast on the substrate and left to dry. Raman spectra were recorded with an Invia Renishaw microspectrometer equipped with a He−Ne laser at 633 nm using the 100× objective. Samples were prepared by drop casting the dispersion on silicon oxide surfaces (Si-Mat silicon wafers, CZ), and the solvent was let to evaporate. For Raman analysis, 30 spectra were taken of each sample.

Sample Preparation. In 30 mL of DMF during 1 h, 10 mg of graphite crystals (Bay Carbon, Inc. (SP-1 graphite powder, www.baycarbon.com) were ultrasonicated in order to induce partial exfoliation of graphite (G-1). After sonication, dispersions were left to stabilize for 5 min, and then the liquid phase was removed by pipetting. Dispersions were copiously washed by filtration with fresh DMF to remove all possibly altered DMF formed during ultrasonication. Special attention was paid to keep the samples wet during the filtration processes. G-1 dispersion was used as starting material for the further experiments. As the control experiment, we performed a 3 h sonication of G-1 without the addition of Fc-CHO (G-DMF). Sonicated DMF was always removed by filtration, and the wet precipitate was redispersed in 10 mL of fresh DMF. Then, in a different set of experiments, 40 mg of Fc-CHO was added to G-1. Dispersions were further sonicated for 3 h, under the same experimental conditions. The resulting dispersions are named D-Fc-CHO. This product was copiously washed by filtration with fresh DMF in order to remove Fc-CHO and byproduct molecules. Samples were redispersed in a bath ultrasonicator (few seconds) in 10 mL of fresh DMF. Centrifugation of all dispersions was carried out at 3000 rpm for 30 min. A precipitate was observed only for G-1. Two liquid fractions, of 5 mL each, of the D-Fc-CHO dispersion were collected and analyzed.

■ ASSOCIATED CONTENT

Supporting Information

Figures: (1) MWNT formation on the edges of graphene layers; (2) HR-TEM of graphene edges and MWNTs formation; (3) MWNTs produced by the addition on Fc-CHO mixed with graphene layers; (4) G-Fc-CHO; (5) O1s peak of D-Fc-CHO; (6) Control experiment Fc; (7) control experiment by adding benzaldehyde; (8) control experiment by adding Fc and benzaldehyde; (9) control experiment by adding Fc-COOH; (10) control experiment by adding Fc-CON-$(CH_3)_2$; (11) minimum energy path (MEP) for the rolling up of the graphene nanoribbon in the absence and in the presence of four Fc-CHO molecules; (12) representative snapshots during rolling up of the graphene nanoribbon in the absence and in the presence of four Fc-CHO molecules; (13) MWNTs after annealing treatment; and (14) isosurfaces spin densities of Fc-CHO and Fc radical molecules. Tables: (1) Energy barrier for a SWNT (8,8) rolling up with different number of Fc-CHO molecules; and (2) electron affinities. This material is available free of charge via the Internet at http://pubs.acs.org.

■ AUTHOR INFORMATION

Corresponding Author

mildred@ifisica.uaslp.mx; P.Rudolf@rug.nl; francesco.zerbetto@unibo.it; prato@units.it

Present Address

[⊥]Instituto de Física, Universidad Autonoma de San Luis Potosi, Manuel Nava 6, Zona Universitaria 78290, San Luis Potosi, SLP, Mexico.

Notes

The authors declare no competing financial interest.

■ ACKNOWLEDGMENTS

This work was supported by the University of Trieste, the Italian Ministry of Education MIUR (cofin Prot. 20085M27SS), the European Union through the ERC grant No. 246791 − COUNTATOMS, the grant agreement for an Integrated Infrastructure Initiative N. 262348 ESMI, and the "Graphene-based electronics" research program of the Foundation for Fundamental Research on Matter (FOM).

■ REFERENCES

(1) Rao, C. N. R.; Seshadri, R.; Goviandaraj, A.; Sen, R. *Mater. Sci. Eng., R* **1995**, *15*, 209−262.

(2) Novoselov, K. S.; Geim, A. K.; Morozov, S. V.; Jiang, D.; Zhang, Y.; Dubonos, S. V.; Grigorieva, I. V.; Firsov, A. A. *Science* **2004**, *306*, 666−669.

(3) Meyer, J. C.; Geim, A. K.; Katsnelson, M. I.; Novoselov, K. S.; Booth, T. J.; Roth, S. *Nature* **2007**, *446*, 60−63.

(4) Castro, N.; Guinea, F.; Peres, N. M. R.; Novoselov, K. S.; Geim, A. K. *Rev. Mod. Phys* **2009**, *81*, 109−162.

(5) Frank, I. W.; Tanenbaum, D. M.; van der Zande, A. M.; McEuen, P. L. *J. Vac. Sci. Technol.* **2007**, *25*, 2558−2561.

(6) Geim, A. K.; Novoselov, K. J. *Nat. Mater.* **2007**, *6*, 183−191.

(7) Chuvilin, A.; Kaiser, U.; Bichoutskaia, E.; Besley, N. A.; Khlobystov, A. N. *Nat. Chem.* **2010**, *2*, 450−453.

(8) Joumet, C.; Maser, W. K.; Bernier, P.; Loiseau, A.; Lamy de la Chapelle, M.; Lefrant, S.; Deniard, P.; Lee, R.; Fischer, J. E. *Nature* **1997**, *388*, 756−758.

(9) Terrones, M. *Int. Mater. Rev.* **2004**, *49*, 325−377.

(10) Hafner, J. H.; Bronikowski, M. J.; Azamian, B. R.; Nikolaev, P.; Rinzler, A. G.; Colbert, D. T.; Smith, K. A.; Smalley, R. E. *Chem. Phys. Lett.* **1998**, *296*, 195−202.

(11) Haddon, R. C.; Sippel, J.; Rinzler, A. G.; Papadimitrakopoulos, F. *MRS Bull.* **2004**, *29*, 252−259.

(12) Skrabalak, S. E. *Phys. Chem. Chem. Phys.* **2009**, *11*, 4930−4942.

(13) Kaempgen, M.; Lebert, M.; Haluska, M.; Nicolso, N.; Roth, S. *Adv. Mater.* **2008**, *20*, 616−620.

(14) Jeong, S.-H.; Ko, J.-H.; Park, J.-B.; Park, W. J. *J. Am. Chem. Soc.* **2004**, *126*, 15982−15983.

(15) Li, C. P.; Teo, B. K.; Sun, X. H.; Wong, N. B.; Lee, S. T. *Chem. Mater.* **2005**, *17*, 5780−5788.

(16) Li, C.-P.; Wong, N.-B.; Lee, C.-S.; Lee, S.-T.; Teo, B. K. *J. Am. Chem. Soc.* **2002**, *124*, 14856−14857.

(17) Hernandez, Y.; Nicolosi, V.; Lotya, M.; Blighe, F. M.; Sun, Z.; De, S.; McGovern, I. T.; Holland, B.; Byrne, M.; Gun'Ko, Y. K.; Boland, J. J.; Niraj, P.; Duesberg, G.; Krishnamurthy, S.; Goodhue, R.; Hutchison, J.; Scardaci, V.; Ferrari, A. C.; Coleman, J. N. *Nat. Nanotechnol.* **2008**, *3*, 563−568.

(18) Shin, C.-J.; Lin, S.; Strano, M. S.; Blankschtein, D. *J. Am. Chem. Soc.* **2010**, *132*, 14638−14648.

(19) Cravotto, G.; Cintas, P. *Chem.—Eur. J.* **2010**, *16*, 5246−5259.

(20) Gedanken, A. *Ultrason. Sonochem.* **2004**, *11*, 47−55.

(21) Suslick, K. S.; Choe, S.-B.; Cichowlas, A. A.; Grinstaff, M. W. *Nature* **1991**, *353*, 414−416.

(22) Khan, U.; ÓNeil, A.; Loyta, M.; De, S.; Coleman, J. N. *Small* **2010**, *6*, 864−871.

(23) Misik, V.; Riesz, P. *Free Radical Biol. Med.* **1996**, *20*, 129−138.
(24) Wang, J.; Huang, L. Y.; Chen, G. A.; Huang, J. L. *Chem. Lett.* **2005**, *34*, 1514−1515.
(25) Fukuzimi, S.; Shimoosako, K.; Suenobu, T.; Watanabe, Y. *J. Am. Chem. Soc.* **2003**, *125*, 9074−9082.
(26) Cao, A.; Dickerel, P. L.; Sawyer, W. G.; Ghasemi-Nejhad, M. N.; Ajayan, P. M. *Science* **2005**, *310*, 1307−1310.
(27) Ugarte, D. *Nature* **1992**, *359*, 707−709.
(28) Kosaka, M.; Ebbesen, T. W.; Hiura, H.; Tanigaki, K. *Chem. Phys. Lett.* **1995**, *233*, 47−51.
(29) Iijima, S. *Nature* **1991**, *354*, 56−58.
(30) Zhang, X. F.; Zhang, X. B.; Van Tendeloo, G.; Amelinckx, S.; Op de Beeck, M.; Van Landuyt, J. *J. Cryst. Growth* **1993**, *130*, 368−382.
(31) Berber, S.; Tománek, D. *Phys. Rev. B* **2004**, *69*, 233404.
(32) Ferrari, A. C.; Robertson, J. *Phys. Rev. B* **2000**, *61*, 14095−14107.
(33) Meyer, J. C.; Geim, A. K.; Katsnelson, M. I.; Novoselov, K. S.; Obergfell, D.; Roth, S.; Girit, C.; Zettl, A. *Solid State Commun.* **2007**, *143*, 101−109.
(34) Ferrari, A. C.; Meyer, J. C.; Scardaci, V.; Casiraghi, C.; Lazzeri, M.; Mauri, F.; Piscanec, S.; Jiang, D.; Novoselov, K. S.; Roth, S.; Geim, A. K. *Phys. Rev. Lett.* **2006**, *97*, 187401.
(35) Subrahmanyam, K. S.; Vivekch, S. R. C.; Govindaraj, A.; Rao, C. N. R. *J. Mater. Chem.* **2008**, *18*, 1517−1523.
(36) Shah, Y. T.; Pandit, A. B.; Moholkar, V. S. In *Cavitation Reaction Engineering (Plenum Chemical Engineering Series)*; Kluwer Academic/Plenum Publishers: New York, 1999.
(37) Ramanathan, T.; Abdala, A. A.; Stankovich, S.; Dikin, D. A.; Herrera-Alonso, M.; Piner, R. D.; Adamson, D. H.; Schniepp, H. C.; Chen, X.; Ruoff, R. S.; Nguyen, S. T.; Aksay, I. A.; Prud'Homme, R. K.; Brinson, L. C. *Nat. Nanotech.* **2008**, *3*, 327−331.
(38) Yu, D.; Liu, F. *Nano Lett.* **2007**, *7*, 3046−3050.
(39) Bets, K. V.; Yakobson, B. I. *Nano Res.* **2009**, *2*, 161−166.
(40) Gass, M. H.; Bangert, U.; Bleloch, A. L.; Wang, P.; Nair, R. R.; Geim, A. K. *Nat. Nanotechnol.* **2008**, *3*, 676−681.
(41) Ivanovskaya, V. V.; Zobelli, A.; Wagner, P.; Heggie, M. I.; Briddon, P. R.; Rayson, M. J.; Ewels, C. P. *Phys. Rev. Lett.* **2011**, *107*, 065502.
(42) Plank, W.; Pfeiffer, R.; Schaman, C.; Kuzmany, H.; Calvaresi, M.; Zerbetto., F.; Meyer, J. *ACS Nano* **2010**, *4*, 4515−4522.
(43) Zhu, J.; Sun, K.; Sim, D.; Xu, C.; Zhang, H.; Hng, H. H.; Yan, Q. *Chem. Commun.* **2011**, *47*, 10383−10385.
(44) Sharma, R.; Huun, B.; Perera., C. J.; Strano, M. S. *Nano Lett.* **2010**, *10*, 398−405.
(45) Klusek, Z.; Kozlowski, W.; Waqar, Z.; Datta, S.; Burnell-Gray, J. S.; Makarenko, I. V.; Gall, N. R.; Rutkov, E. V.; Tontegode, A. Y.; Titkov, A. N. *Appl. Surf. Sci.* **2005**, *252*, 1221−1227.
(46) Wimmer, M.; Akhmerov, A. R.; Guinea, F. *Phys. Rev. B* **2010**, *82*, 045409.
(47) Moulder, J. K.; Stickle, W. F.; Sobol, P. E.; Bomben, K. D. In *Handbook of X-ray photoelectron Spectroscopy*; Minnesota, 1992.